

Measurements of thermal transport in low stress silicon nitride films

W. Holmes,^{a)} J. M. Gildemeister, and P. L. Richards^{b)}

Physics Department, University of California, Berkeley, California 94720

and Materials Sciences Division, Lawrence Berkeley National Laboratory, Berkeley, California 94720

V. Kotsubo^{c)}

Conductus, Inc., Sunnyvale, California 94440

(Received 3 February 1998; accepted for publication 4 March 1998)

We have measured the thermal conductance, G , of $\approx 1 \mu\text{m}$ thick low stress silicon nitride membranes over the temperature range, $0.06 < T < 6 \text{ K}$, as a function of surface condition. For $T > 4 \text{ K}$, G is independent of surface condition indicating that the thermal transport is determined by bulk scattering. For $T < 4 \text{ K}$, scattering from membrane surfaces becomes significant. Membranes which have submicron sized Ag particles glued to the surface or are micromachined into narrow strips have a G that is reduced by a factor as large as 5 compared with that of clean, solid membranes with the same ratio of cross section to length. © 1998 American Institute of Physics. [S0003-6951(98)02318-3]

Low stress silicon nitride (Si–N) membranes are being used in a variety of devices at or below liquid helium temperatures. These include bolometric millimeter-wave detectors^{1–3} used for ground based and balloon borne astronomical telescopes and proposed for the space astronomy missions FIRST and Planck. Other applications include x-ray calorimeters,⁴ tunnel junction refrigerators,^{5,6} superfluid helium devices,⁷ and microcalorimeters.⁸ The thermal conductance, G , of the Si–N membrane is a critical design parameter for many of these applications, but is difficult to measure because it is usually very small.

In crystalline insulators at high temperatures, values of the phonon mean free path, $\ell_{\text{eff}} = 3\kappa/cv_s$, are very short and limited primarily by Umklapp processes. Here κ is the thermal conductivity, c is the specific heat per unit volume, and v_s is the average sound speed. At temperatures lower than $\approx 20 \text{ K}$, Umklapp processes decrease dramatically and impurity or dislocation scattering dominates. In amorphous materials, such as low stress Si–N membranes, ℓ_{eff} is approximately a lattice spacing at high temperatures and is limited by scattering from disorder. In both crystalline and amorphous materials, the dominant phonon wavelengths, $\lambda_d \propto 1/T$, increase with decreasing temperature. Therefore, scattering becomes less effective at very low temperatures and ℓ_{eff} increases. At sufficiently low temperatures, ℓ_{eff} can exceed sample dimensions, so phonon surface scattering is important.

A model analogous to radiative transfer between two blackbodies has been used to describe thermal transport in the surface scattering limit in crystalline dielectric samples a few millimeters^{9,10} to a few microns in thickness.^{11,12} The heat flow can be written $G = 4\sigma AT^3\xi$, where A is the cross sectional area of the membrane perpendicular to the direction of heat flow and $\sigma = \sum_i (\pi^5 k_B^4 / 15h^3 v_i^2) = 15.7 \text{ mW/cm}^2 \text{ K}^4$

is the Stefan–Boltzmann constant obtained by summing over the two transverse and one longitudinal acoustic modes which have sound speeds of $v_t = 6.2 \times 10^5$ and $v_l = 10.3 \times 10^5 \text{ cm/s}$, respectively, in similar Si–N membranes.¹³ The numerical factor $\xi < 1$ gives the reduction in G due to diffuse surface scattering. An upper limit to G is obtained for the case of specular surface scattering where $\xi = 1$. A lower limit, known as the Casimir limit, is obtained for the case of complete diffuse surface scattering.^{14,15} Phonons hitting the sample surface are assumed to scatter into all solid angles. For the case of wafers of crystalline insulators in the surface scattering limit, a reduction of G has been observed when the surface was damaged or when a thin film was deposited on the surface.^{9,10} In this paper, we use these ideas to understand data on the thermal conductance of amorphous Si–N membranes.⁸

Our experimental configuration is shown in Fig. 1. The ring of membrane with width $\Delta R = 200 \mu\text{m}$ is defined by $1 \mu\text{m}$ thick metal (Pt or Au) films which are essentially isothermal. The central disk of radius R is equipped with a heater and a thermometer which are $240 \mu\text{m}$ cubes of neutron transmutation doped (NTD) Ge with ion implanted and metallized contacts.¹⁶ Low thermal conductance leads are made from commercial¹⁷ $25 \mu\text{m}$ diameter Cu clad Nb–Ti superconducting wire attached to the NTD Ge with Ag filled epoxy.¹⁸ The Cu cladding was removed by etching over a 5 mm central segment of each lead. Graphite fibers¹⁹ were used for some early experiments, but were inconvenient because of their high electrical resistance. A commercial Ge thermometer²⁰ in good thermal contact with the outer metal film was used to measure its temperature and also to calibrate the NTD Ge thermometer. The temperature dependence of the NTD Ge is in excellent agreement with the dependence $R = R_0 \exp(\sqrt{T_0/T})$ expected for phonon assisted variable range hopping. Thermometers with R_0 , T_0 of 12Ω , 52 K and 7Ω , 21 K proved useful for our temperature range. Both the thermometer and the heater were current biased. The voltages were read out with differential source follower circuits, each using an InterFET NJ132 JFET cooled to 120 K

^{a)}Permanent address: Department of Chemistry, Stanford, CA 94305.

^{b)}Electronic mail: richards@physics.berkeley.edu

^{c)}Permanent address: Lockheed-Martin Marietta, 4041 N. First St., San Jose, CA 95134.

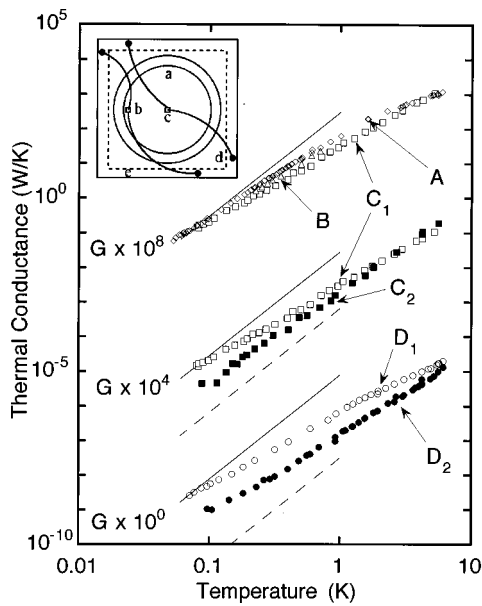


FIG. 1. The measured thermal conductance as a function of temperature of six membranes plotted on a log-log scale. Sets of values of G have been multiplied by 10^4 and 10^8 to separate them for clarity. The specular limit, plotted as a solid line is a good fit to the low temperature data on bare membranes A , B , C_1 , and D_1 . The Casimir limit plotted as a dashed line lies below the data for all membranes. The sample configuration is shown in the inset. The isothermal metallized disk a has thermometer b and heater c attached. Together with metallized region d , it defines the measured Si-N ring. The free standing Si-N membrane (inside the dashed line) is supported by a Si picture frame e . The thermometer and heater lead wires are anchored to insulated contact pads.

for reduced noise. The thermometer, lead, and readout techniques used here were adapted from conventional infrared bolometer technology.²¹

The precision and reproducibility of our measurements of the membrane thermal conductance G was repeatedly checked and found to be better than 5%. Absolute accuracy of the same level was obtained by choosing an experimental configuration where the membrane G is large compared to the parallel conductance of the leads and small compared to all series conductances. The thermal conductance, G_l , of the leads was measured by completely removing the ring of membrane leaving the center metallized disk supported only by the leads. The measured values of G_l are in agreement with published values for Nb-Ti.²² Corrections to the raw G measurements of $\approx 15\%$ were made at the lowest temperatures where G_l becomes significant. The thermal conductances of the metal films were obtained from the Wiedemann-Franz law and measurements of the low temperature resistance of witness samples. Thermal gradients in the films were just significant at 6 K so no corrections were required. The gradients due to the electron-phonon coupling in the metal are very small in our samples.²³ Heat is transferred between the metal and the membrane over a strip of width $\approx \sqrt{G/g_b}$, where $g_b \approx 50 \text{ T}^3 \text{ mW/K cm}^2$ is the boundary conductance.²⁴ Estimated corrections to the raw G are $< 3\%$ so none were made.

Low stress Si-N was grown on both sides of a (100) Si wafer by low pressure chemical vapor deposition at the UC Berkeley Microfabrication Laboratory.¹³ The $1 \mu\text{m}$ Au films with 5 nm Mo adhesion layers were deposited by e -beam evaporation and patterned by liftoff. The $1 \mu\text{m}$ Pt films with

TABLE I. Dimensions and properties of several membranes.

Sample	t μm	R mm	A cm^2	$A/\Delta R$ cm	Membrane condition
A	0.85	0.9	4.8×10^{-5}	2.7×10^{-3}	bare
B	0.85	0.9	4.8×10^{-5}	2.7×10^{-3}	bare
C_1	0.79	0.9	4.5×10^{-5}	2.5×10^{-3}	bare
C_2	0.79	0.9	4.5×10^{-5}	2.5×10^{-3}	Ag particles
D_1	1.02	1.9	12×10^{-5}	6.4×10^{-3}	bare
D_2	1.02	1.9	6.1×10^{-5}	3.2×10^{-3}	spokes

5 nm Ti adhesion layers were deposited by sputtering and patterned by etching in aqua regia. The Si was etched from the back side using KOH to leave free standing membranes. The Si-N ring on sample D_2 was etched into radial spokes by a SF_6 plasma. Individual spokes are $\approx 5 \mu\text{m}$ wide, separated by spaces $\approx 5 \mu\text{m}$ wide. The cubes of NTD Ge, with leads attached, were glued to the metal using Ag epoxy. The leads were bent, to relieve strain during thermal contraction, and glued to contact pads with Ag epoxy. We glued submicron sized Ag particles to the backside of sample C_1 to produce C_2 by dispersing ground, cured Ag epoxy in acetone, transferring drops to the membrane and allowing the solvent to evaporate after each drop. In this way a haze was produced that was visible through the ring on the front side. A scanning electron microscope was used to determine that the particle diameters were $\approx 100 \text{ nm}$ and the density was $\approx 10 \text{ particles}/\mu\text{m}^2$.

The measured values of G for the samples described in Table I are shown in Fig. 1. We divide by the numerical factor $A/\Delta R$ given in Table I to obtain values of the effective thermal conductivity, κ_{eff} . We then compute an effective mean free path $\ell_{\text{eff}} = 3 \kappa_{\text{eff}} / c v_s$ using the bulk specific heat²⁵ $c = 0.58 \text{ T}^3 \mu\text{J/K cm}^3$, which is compatible with the Debye model and sound velocities for Si-N membranes.¹³ When surface scattering is important, values of ℓ_{eff} obtained in this way are a lower limit to the ℓ determined by bulk scattering.

At our highest temperatures, $4 < T < 6 \text{ K}$, we find comparable values of κ_{eff} for all samples which are consistent with those of thick samples of other amorphous materials. Values of ℓ_{eff} are $\approx t$. We conclude that bulk scattering dominates for $T > 4 \text{ K}$. At lower temperatures, ℓ_{eff} becomes 10–100 times larger than t clearly indicating the importance of surface scattering. For example, our ℓ_{eff} is ≈ 3 times larger than that of bulk amorphous SiO_2 at 4 K, but rises less rapidly with decreasing temperature since surface scattering begins to dominate.

In Fig. 1, we compare measured values of $G(T)$ with the specular and Casimir limits of surface scattering. The values for bare membranes A , B , C_1 , and D_1 all approach the specular limit for $T < 0.2 \text{ K}$ where λ_d becomes very large. There are small, reproducible differences in G/A at intermediate temperatures which may be due to unintentional surface contamination. Sample C_1 was measured bare, and then remeasured as C_2 after Ag particles were deposited. Below 4 K, these data unambiguously show that G is reduced by changes in the membrane surface. If bulk diffusion was dominant, addition of material on the surface would provide a parallel heat flow path and increase G . This result was

confirmed by removing Ag particles on another membrane by plasma etching and observing that G increased and by evaporating a 10 nm thick Au film on a membrane which caused G to decrease.

The spoked sample D_2 is compared with a nominally identical sample with a continuous membrane. The cross section A is a factor of 2 smaller for D_2 due to the removal of material between the spokes but G has been reduced by a factor as large as 10. This result is consistent with an observation in the literature of a surprisingly small G in long, narrow, micromachined Si-N strips.²

The Casimir limit for D_2 is obtained from the approximation $\xi \approx \sqrt{A}/\Delta R$ which is valid for an individual spoke where $\sqrt{A}/\Delta R \ll 1$. For the other samples, the aspect ratio, $R/t \gg 1$, is large so the value of ξ is obtained using an expression in Wyebourne *et al.*^{15,26} The Casimir limit is not reached in any of our samples or in crystalline Si membranes with thicknesses of several microns measured by others.¹² However, the Casimir limit was reached in crystalline Si with thicknesses of a few millimeters by sandblasting the surface which produces microcracks.¹⁰ One explanation of why complete diffuse scattering has not been seen in membranes is that the size of surface cracks must be $\approx \lambda_d \approx 75/T$ nm to effectively scatter phonons. Below 1 K, λ_d approaches t . Therefore, the scattering centers must be comparable in size to t to produce complete diffuse phonon scattering. Microcracks with dimensions of order t would probably cause a membrane to break. Our Ag particle scattering centers were small compared with t .

We have studied the thermal transport in low stress silicon nitride membranes at temperatures $0.06 < T < 6$ K and as a function of surface condition. Bulk phonon scattering dominates above 4 K. Below 4 K specular and diffuse phonon surface scattering must be considered. Diffuse surface scattering was produced both by surface contamination and by micromachining long narrow features as are required in many device applications.

The authors thank Professor T. W. Kenny, Professor S. Watson, and Professor F. Hellman for valuable input concerning the analysis of our data. This work was supported in

part by the Director, Office of Energy Research, Office of Basic Energy Sciences, Materials Sciences Division of the U.S. Department of Energy under Contract No. DE-AC03-76SF00098.

- ¹E. Kreysa, J. Beeman, and E. Haller, in *The 30th ESLAB Symposium on Submillimeter and Far-Infrared Space Instrumentation*, edited by E. Rolfe (ESA Publications Division, ESTEC, Noordwijk, The Netherlands, 1996), pp. 111–114.
- ²P. D. Mauskopf, J. J. Bock, H. Del Castillo, W. L. Holtzapfel, and A. E. Lange, *Appl. Opt.* **36**, 765 (1997).
- ³D. Osterman, R. Patt, R. Hunt, and J. Peterson, *Appl. Phys. Lett.* **71**, 2361 (1997).
- ⁴K. D. Irwin, G. Hilton, D. Wollman, and J. M. Martinis, *Appl. Phys. Lett.* **69**, 1945 (1996).
- ⁵M. Nahum, T. M. Eiles, and J. M. Martinis, *Appl. Phys. Lett.* **65**, 3123 (1994).
- ⁶A. J. Manninen, A. Leivo, and J. P. Pekola, *Appl. Phys. Lett.* **70**, 1885 (1997).
- ⁷K. Schwab, N. Bruckner, and R. E. Packard, *Nature (London)* **386**, 585 (1997).
- ⁸D. W. Denlinger, E. N. Abarra, K. Allen, P. W. Rooney, M. T. Messer, S. K. Watson, and F. Hellman, *Rev. Sci. Instrum.* **65**, 943 (1994).
- ⁹R. Berman, E. Foster, and J. M. Ziman, *Proc. R. Soc. London, Ser. A* **231**, 130 (1955).
- ¹⁰T. Klitsner and R. O. Pohl, *Phys. Rev. B* **36**, 6551 (1987).
- ¹¹P. Downey, A. D. Jefferies, S. S. Meyer, R. Weiss, F. J. Bachner, J. P. Donnelly, W. T. Lindley, R. W. Mountain, and D. J. Silversmith, *Appl. Opt.* **23**, 910 (1984).
- ¹²S. Moseley (unpublished).
- ¹³S. Wenzel, Ph.D. thesis, University of California at Berkeley, 1992.
- ¹⁴H. Casimir, *Physica (Amsterdam)* **5**, 495 (1938).
- ¹⁵M. Wyebourne, C. Eddison, and M. Kelly, *J. Phys. C: Condens. Matter* **17**, L607 (1984).
- ¹⁶E. E. Haller, *Infrared Phys.* **25**, 257 (1985).
- ¹⁷Cu clad Nb-Ti wire, California Fine Wire, 338 S. Fourth St., Grover Beach, CA 93433-1999.
- ¹⁸H20E Epoxy, Epoxy Technologies, Billerica, MA 02154.
- ¹⁹Graphite Fiber, Hercules Aerospace Co., P.O. Box 98, Magna, UT 84044.
- ²⁰Lake Shore Cryotronics, Inc., 64 E. Walnut St., Westerville, OH 43081; Model GRT-200.
- ²¹P. Richards, *J. Appl. Phys.* **76**, 1 (1994).
- ²²J. R. Olson, *Cryogenics* **33**, 729 (1993).
- ²³F. C. Wellstood, C. Urbina, and J. C. Clarke, *Phys. Rev. B* **49**, 5942 (1994).
- ²⁴W. Little, *Can. J. Phys.* **37**, 334 (1959).
- ²⁵V. Koshchenko, A. Pashinkin, V. Yachmenev, and A. Lephov, *Proc. USSR Acad. Sci.* **11**, 3073 (1981).
- ²⁶In terms of the phonon mean free path calculated for the Casimir limit, ℓ_B , by Wyebourne *et al.*, the parameter $\xi = 3\ell_B/4\Delta R$.